

Exploring Negatives in Contrastive Learning for Unpaired Image-to-Image Translation

Yupei Lin*

Guangdong University of Technology
Guangzhou, China
yupeilin2388@gmail.com

Sen Zhang*

The University of Sydney
Sydney, Australia
szha2609@uni.sydney.edu.au

Tianshui Chen

Guangdong University of Technology
Guangzhou, China
tianshuichen@gmail.com

Yongyi Lu

Guangdong University of Technology
Guangzhou, China
yylu1989@gmail.com

Guangping Li

Guangdong University of Technology
Guangzhou, China
gpli@gdut.edu.cn

Yukai Shi[†]

Guangdong University of Technology
Guangzhou, China
ykshi@gdut.edu.cn

ABSTRACT

Unpaired image-to-image translation aims to find a mapping between the source domain and the target domain. To alleviate the problem of the lack of supervised labels for the source images, cycle-consistency based methods have been proposed for image structure preservation by assuming a reversible relationship between unpaired images. However, this assumption only uses limited correspondence between image pairs. Recently, contrastive learning (CL) has been used to further investigate the image correspondence in unpaired image translation by using patch-based positive/negative learning. Patch-based contrastive routines obtain the positives by self-similarity computation and recognize the rest patches as negatives. This flexible learning paradigm obtains auxiliary contextualized information at a low cost. As the negatives own an impressive sample number, with curiosity, we make an investigation based on a question: are all negatives necessary for feature contrastive learning? Unlike previous CL approaches that use negatives as much as possible, in this paper, we study the negatives from an information-theoretic perspective and introduce a new negative Pruning technology for Unpaired image-to-image Translation (PUT) by sparsifying and ranking the patches. The proposed algorithm is efficient, flexible and enables the model to learn essential information between corresponding patches stably. By putting quality over quantity, only a few negative patches are required to achieve better results. Lastly, we validate the superiority, stability, and versatility of our model through comparative experiments.

CCS CONCEPTS

• **Computing methodologies** → **Image representations**; **Un-supervised learning**; **Feature selection**.

KEYWORDS

contrastive learning, image-to-image translation, generative adversarial network

ACM Reference Format:

Yupei Lin, Sen Zhang, Tianshui Chen, Yongyi Lu, Guangping Li, and Yukai Shi. 2022. Exploring Negatives in Contrastive Learning for Unpaired Image-to-Image Translation. In *Proceedings of the 30th ACM International Conference on Multimedia (MM '22)*, October 10–14, 2022, Lisboa, Portugal. ACM, New York, NY, USA, 9 pages. <https://doi.org/10.1145/nnnnnnnn.nnnnnnn>

1 INTRODUCTION

The image-to-image translation task aims to match the style of images from a source domain into a target domain, while retaining the original structure of the source images [3, 22, 36]. For current unpaired image-to-image translation datasets, the generative adversarial nets (GAN) [9, 23, 30, 40, 43] are able to generate images that match the style, but the adversarial loss suffers from the collapse of the structure. This problem may lead to translated images with poor qualities. Thus, improving the quality of image translation with consistent structure remains a very challenging task.

To alleviate this problem, a family of methods based on cycle-consistency learning [3, 8, 11, 21, 44] have been proposed. Cycle-consistency assumes that there exists a reversible relationship between the source image and the target image. Taking advantage of this relationship, the generative adversarial network can preserve the consistency of the image structure. Nevertheless, this assumption has a limited flexibility, since the cyclic loss solely imposes strict alignment on the structures without exploiting other knowledge.

Recently, CUT [27] refreshes the cycle-consistent paradigm by incorporating contrastive learning (CL) into unpaired image-to-image (I2I) translation. By using CL, the generative model is able to use auxiliary knowledge to complement the cycle-consistency. As shown in Fig. 1, given a query sample, CUT chooses to use an assigned patch (i.e., in the same location) as the positive target for cycle-consistent learning. Meanwhile, CUT cleverly uses non-local image structures as the negative samples. This flexible learning

*Both authors contributed equally to this research.

[†]Corresponding author: Yukai Shi

Permission to make digital or hard copies of all or part of this work for personal or classroom use is granted without fee provided that copies are not made or distributed for profit or commercial advantage and that copies bear this notice and the full citation on the first page. Copyrights for components of this work owned by others than the author(s) must be honored. Abstracting with credit is permitted. To copy otherwise, to republish, to post on servers or to redistribute to lists, requires prior specific permission and/or a fee. Request permissions from permissions@acm.org.

MM '22, October 10–14, 2022, Lisboa, Portugal

© 2022 Copyright held by the owner/author(s). Publication rights licensed to ACM.

ACM ISBN 978-x-xxxx-xxxx-x/YY/MM...\$15.00

<https://doi.org/10.1145/nnnnnnnn.nnnnnnn>

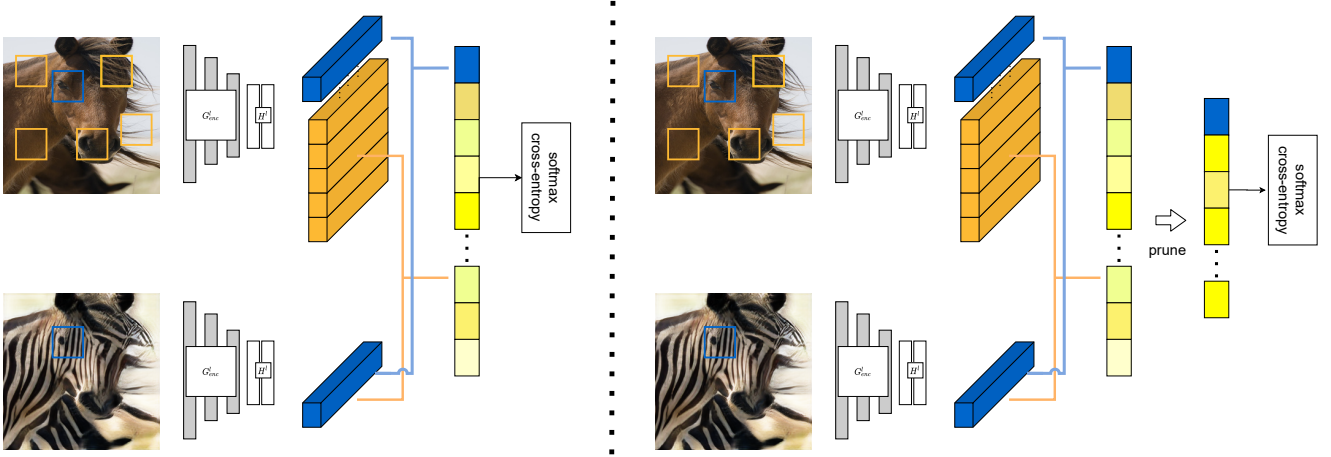


Figure 1: Left: The PatchNCE loss [27]. Right: the proposed RankNCE loss. A typical patch-wise contrastive paradigms usually maximize the mutual information on all the samples, regardless of positive or negative. In comparison, RankNCE selects negative samples with good qualities based on their contribution to the mutual information (MI).

paradigm achieves high-quality image translation without any auxiliary supervision on the training image. However, CUT uses all non-local patches as negative samples, which leads to an obvious problem, i.e., a large number and a potentially high quality diversity of the negative samples. As a result, NEGCUT [35] points out that such unbalanced distribution of negative samples may increase the difficulty of learning, since the information of more relevant negative samples may be overwhelmed by the others. To address this phenomenon, NEGCUT develops a generator to produce fake negative samples. However, NEGCUT still suffers from drawbacks such as the additional computation cost, conflicting quality of negatives, and the increased training difficulty. These problems motivate us to develop an efficient yet advantageous negative selection strategy to learn the essential correspondence between samples.

As suggested in [33], in CL, a uniformity property is usually desired for the features to maintain as much information as possible, which means the high-dimensional features are expected to uniformly distributed on a hypersphere. In this sense, introducing too many negative pairs with diverse qualities in contrastive representation learning would go against this uniformity property. Inspired by RankSRGAN [41], we propose a ranking technology for negative samples, by making the following hypothesis: fewer samples with good quality are enough for CL. Thus, the proposed method attempts to investigate a selective strategy on negative samples. As shown in Fig. 2, to exhibit a discriminative CL, only a few negative patches that contain the most valuable information are carefully preserved. Specifically, we construct negative pruning technology with three steps: i.e., the similarity score computation, pruning, and ranking phrases. In addition, we re-examine PUT in the information-theoretic language to strengthen the interpretability of our method. Overall, the proposed negative pruning technology encourages the generative model to learn essential features, reduces the difficulty of learning, and helps to stabilize training. Our main contributions are:

- Unlike previous contrastive learning methods that use all the negative samples, we investigate strategies to utilize

fewer but better negative samples. Specifically, we develop a negative pruning technology, which consistently shows better results with fewer negative samples.

- To provide further insights and interpretability of our method, we re-examine the image-to-image translation problem from an information-theoretic perspective, by investigating the mutual information between the contrastive pairs.
- In the experiments, we show that PUT brings better superiority and stability. And each sub-component in PUT is carefully analyzed to verify its effectiveness.

The rest of the paper is organised as follows: In Section 2, we present related work, including current methods related to image-to-image translation and contrastive learning. In Section 3, we introduce our methods, including preliminaries and each component of PUT. In Section 4, we present the experimental procedure, the comparison with existing methods, and the results of the ablation experiments. Finally, conclusion and limitations are given in Section 5.

2 RELATED WORK

Image-to-Image (I2I) translation. Image-to-image translation aims to learn the style of images from a source domain into a target domain [1, 19, 31, 35, 37], which can be classified into two groups: the paired setting [18, 18, 28, 34] (supervised) and an unpaired setting (unsupervised). Paired setting means the training set is supervised, each image from source domain has a corresponding label from target domain. Pix2Pix [18], Pix2PixHD [34] and SPADE [28] use adversarial loss [9] in paired training data to train their model. Unlike paired settings, instances of the unpaired setting have no corresponding label from the target domain. To enable to model training with an unsupervised condition, the cycle-consistency has become a popular scheme, which learns a reversible projection from the target domain back to the source domain. For example, UNIT [24], DualGAN [38] and MUNIT [17] train cross-domain GANs with nested cycle-consistent losses. However, this paradigm is often too restrictive to obtain sufficient context. To this end,

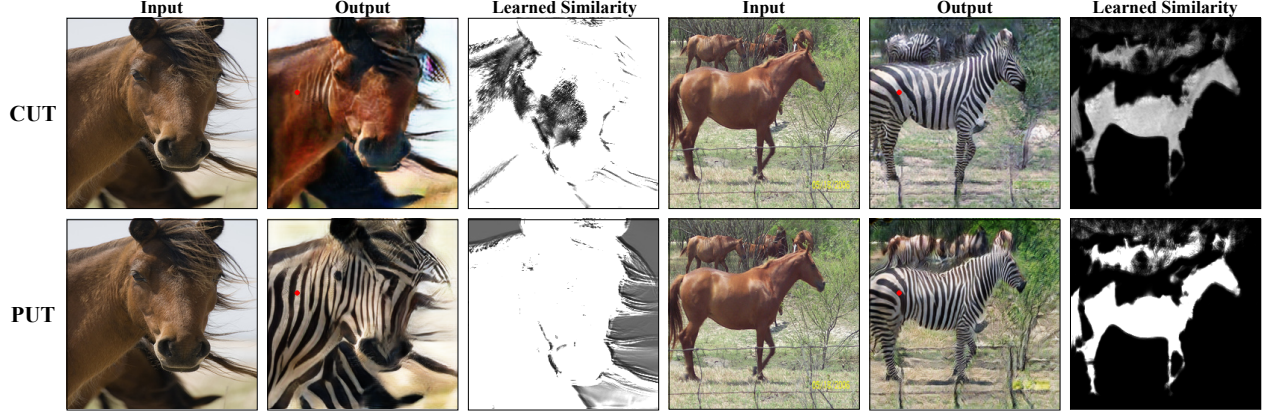


Figure 2: Visualization of the learned similarity by the feature extractor. Given an input and output image, we extract the features of these images through a feature extractor. We compute the learned similarities between the feature vectors of $[(v, v_1^-), \dots, (v, v_N^-)]$ by using $\exp(v \cdot v^- / \tau)$. Specifically, v is a query element (the highlighted red dot in the output) and $[v_1^-, \dots, v_N^-]$ are all the candidate patches in the input. In contrast to CUT, the feature extractor of our model learns the cross-domain correspondence with a better saliency effect.

many approaches attempt to design a unidirectional translation to eliminate the cycle-consistent constraint [26]. DistanceGAN [2] proposes a distance constraint that allows unsupervised domain mapping to be one-sided. GC-GAN [6] enforces geometry consistency as a constraint for unsupervised domain mapping. In recent method, CUT [27] introduces contrast learning in unpaired settings. CUT [27] introduces contrast learning to obtain auxiliary negative labels. However, these methods still suffer from a potentially large number of negative samples with diverse qualities.

Contrastive representation learning. Contrastive learning is a powerful scheme for self-supervised representation learning. It has achieved good results in the field of unsupervised representational learning [4, 13, 14, 16, 32]. Contrastive learning uses a noisy contrastive estimation framework [10] to maximize the mutual information of corresponding patches between images by comparing positive pairs with negative pairs. PatchNCE [27] proposes patch-based contrastive learning, which uses a noise-contrastive estimation framework in unpaired I2I translation tasks by learning the correspondence between the patches of the input image and the corresponding generated image patches. Excellent results are achieved and the recent methods also obtained better performance by utilizing the idea of patch-wise learning. DCLGan [12] uses contrastive loss with a dual-way setting, F-LSeSim[42] proposes a systematic way to obtain a general spatially-correlative map. In parallel to these various designed methods, we mainly investigate negatives sample selection strategies by introducing the idea of ranking in the contrastive learning, which consistently shows better results with fewer negative samples.

3 METHOD

In Fig. 3, we show the architecture of PUT, which includes two types of losses (i.e., adversarial loss and RankNCE loss). In particular, RankNCE is formed by pruning and ranking operations. Firstly, the input image x is mapped by the generator $G : x \rightarrow y$ to generate the image \hat{y} . Secondly, the feature similarity between corresponding patches and non-corresponding patches is calculated at

each layer to obtain mutual information (MI). Finally, top-k patches with the highest similarity are selected by using cross-entropy loss for sorting.

3.1 Preliminaries

Unpaired I2I Translation. Given domain $X \subset \mathcal{R}^{H \times W \times C}$, we hope that the image will be as similar as possible to the image $Y \subset \mathcal{R}^{H \times W \times C}$ with target domain after translation. Given a dataset of unpaired instances $\{x \in X\}$ and $\{y \in Y\}$, the $G : x \rightarrow y$ mapping is completed with a generative network.

To realize the mapping $G : X \rightarrow Y$, we use the adversarial loss to encourage the generative model to produce images that are visually similar to the target domain image. The expression for the adversarial loss is expressed as follows:

$$\mathcal{L}_{GAN}(G, D_Y, X, Y) = E_{y \sim Y} \log D(y) + E_{x \sim X} \log(1 - D(G(x))) \quad (1)$$

PatchNCE. According to contrastive predictive coding [27, 32], a good translated image should have high mutual information with corresponding patches of the input image. To maximize mutual information, PatchNCE [27] employs the contrastive feature learning on internal patches. This loss simply applies a noisy contrastive estimation framework by introducing positive and negative pairs within the image. Specifically, a corresponding positive patch is generated by applying the tokenization step to an input image. And the negative pairs are the patch of the non-corresponding tokens. This method correlates input and output information in a non-local fashion, and the generative model learns rich information from the synergistic/contrastive relationship. Formally, let $v \in \mathcal{R}^C$ denotes the C-dimensional feature vector of the ‘query’ patch, $v^+ \in \mathcal{R}^C$ denotes the feature of the positive patch corresponding to the query patch and $v^- \in \mathcal{R}^{C \times N}$ denotes the features of N negative patches. The contrastive loss is defined as an (N+1)-way classification problem, and is expressed as:

$$\ell(v, v^+, v^-) = -\log\left(\frac{\exp(v \cdot v^+) / \tau}{\exp(v \cdot v^+) / \tau + \sum_{i=1}^N \exp(v \cdot v_i^-) / \tau}\right), \quad (2)$$

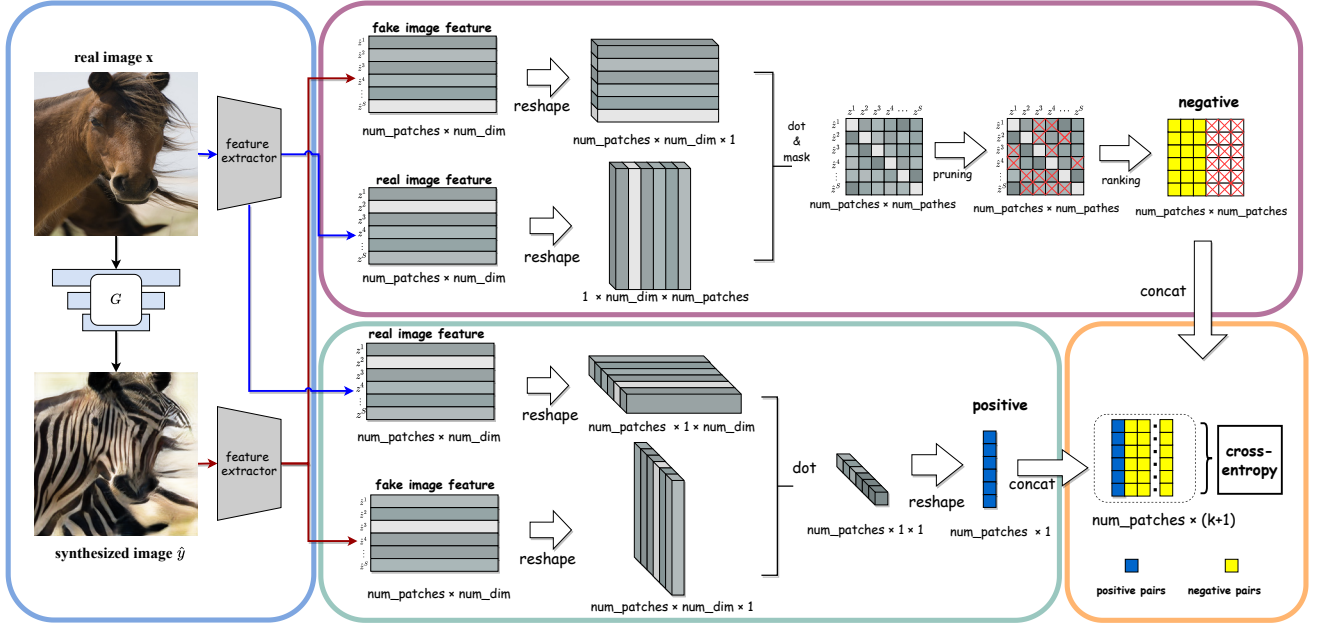


Figure 3: The proposed RankNCE loss. The real images x and the synthesized image \hat{y} are firstly transformed into feature vectors using the generator G . The synergistic relationship is computed by applying dot-product on homogeneous features. The contrastive relationship is obtained by multiplying determinantal features of fake/real images. Our proposed RankNCE differs from existing methods by pruning and ranking rough negatives.

where τ indicates the temperature coefficient, N is the number of negative patches. In Eq. 2, $\tau = 0.07$ and $N = 255$.

3.2 RankNCE

Based on Eq. 2, we review negative samples by observing that the negatives have a large sample number and MI variance. By putting quality over quantity, we attempt to sort out valuable patches to realize a discriminative representation learning under the contrastive paradigm. We therefore modify Eq. 2 by introducing the idea of rank. The RankNCE loss is expressed as:

$$\ell_{\text{rank}}(v, v^+, v^-) = -\log\left(\frac{\exp(v \cdot v^+)/\tau}{\exp(v \cdot v^+)/\tau + \sum_{i=1}^K \exp(r(v \cdot v_i^-, K))/\tau}\right) \quad (3)$$

where $v \cdot v^-$ is the similarity between query patch and negative patch, k is an empirical value for valuable negative sample preserving. And $r(v \cdot v_i^-, K)$ denotes the ranking operator to sort out top- K most similar patches, where $K \ll N$. Especially, the ranking operator contains three-step: *similarity score computation*, *pruning* and *ranking*.

Similarity score computation. Inspired by InfoNCE [32] and PatchNCE [27], we first obtain the similarity scores between the real image and fake images by calculating the dot-product similarities. As shown in Fig. 3, the extracted features of real image and fake image features are $\{z^1, \dots, z^S\} \subset Z$ and $\{\hat{z}^1, \dots, \hat{z}^S\} \subset \hat{Z}$, respectively. We

obtain the similarity score matrix C_{sim} as:

$$\begin{aligned} C_{\text{sim}} &= \hat{Z}^T Z, \\ &= [\hat{z}^1, \dots, \hat{z}^S]^T [z^1, \dots, z^S], \\ \text{mask} &= \begin{bmatrix} 0 & \hat{z}^1 z^2 & \dots & \hat{z}^1 z^S \\ \hat{z}^2 z^1 & 0 & \dots & \hat{z}^2 z^S \\ \dots & \dots & \dots & \dots \\ \hat{z}^S z^1 & \hat{z}^S z^2 & \dots & 0 \end{bmatrix}, \end{aligned} \quad (4)$$

where mask means the diagonal elements are filled with zero.

Pruning. To remove meaningless negative samples that were involved in discriminative learning, we distill C_{sim} by sparsifying elements according to $MI(v||v^-)$. In other words, the local samples, which contribute less to the mutual information between the anchor and its negative samples, are restricted from participating in CL.

Ranking. A ranking operator is then applied in C_{sim} to preserve the most valuable elements. As shown in Fig. 3, the top- K patches with the highest similarity scores are sorted out according to the y-axis, and the remaining negatives are reset to zero. Though we have used ranking operation, the preliminary pruning scheme is necessary, as the sort operation still has an opportunity to retain negative pairs that contribute less to $MI(v||v^-)$.

Finally, the reserved elements in C_{sim} are utilized as negative samples. As shown in Fig. 3, the positive/negative samples are collected for CL with Eq. 3. To further demonstrate the difference between PatchNCE and RankNCE, we compare the learned similarities of each method in Fig. 2. Intuitively, PUT leans the cross-domain correspondence with a better saliency effect, which justify our strategy is helpful to discriminative representation learning. To provide more insights and interpretability of PUT, we further

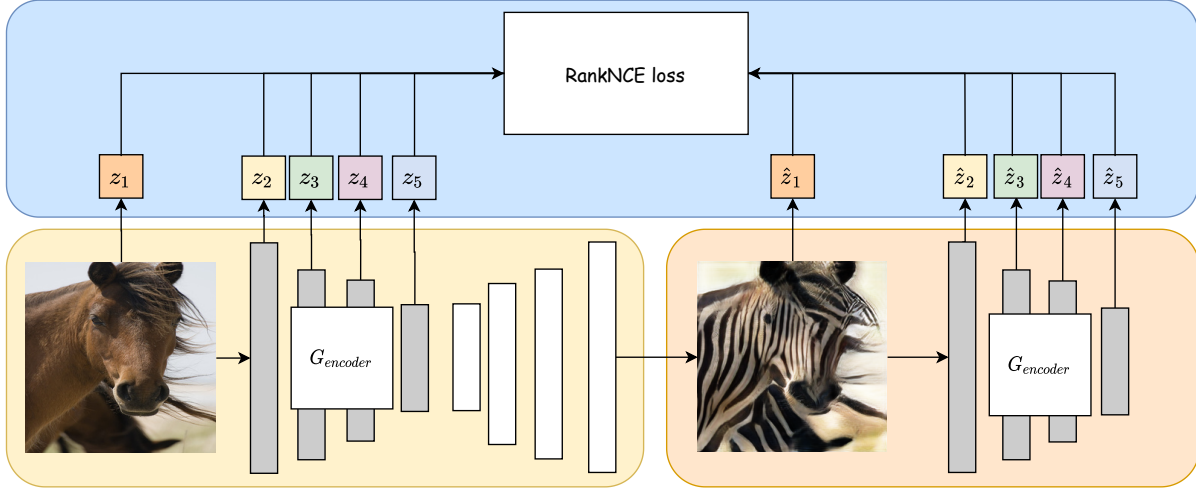


Figure 4: A illustration of multi-layer RankNCE loss.

investigate the MI between the synergistic/contrastive patches from an information-theoretic perspective.

3.3 Information-theoretic Perspective

Intuitively, from the information-theoretic perspective, a good CL approach should maximize the MI between v and v^+ , while minimizing the MI between v and v^- at the same time. It has been shown that minimizing the contrastive loss in Eq. 2 can be regarded as maximizing a variational lower bound of the mutual information $MI(v||v^+)$ between the features of the query patch and its positive pair [29]:

$$MI(v||v^+) \geq E[\log \frac{\exp(v \cdot v^+)/\tau}{\exp(v \cdot v^+)/\tau + \sum_{n=1}^N \exp(v \cdot v_n^-)/\tau}]. \quad (5)$$

Of note is that the lower bound of $MI(v||v^+)$ in Eq. 5 makes the underlying assumption that v^+ and v are both independent from v^- , which will not necessarily hold in practice. Instead, when the independence assumption is violated, we have the following lower bound for the mutual information $MI(v||v^+, v^-)$ between the features of the query patch and its positive/negative pairs [29]:

$$MI(v||v^+, v^-) \geq E[\frac{1}{N+1} \sum_{i=0}^N \log \frac{\exp(v_i \tilde{v}_i^+)/\tau}{\frac{1}{N+1} \sum_{k=0}^N \exp(v_k \tilde{v}_k^+)/\tau}], \quad (6)$$

where $v_0 = v^+$ and $v_i = v_i^-$ for $i \geq 1$. \tilde{v}_i^+ denotes the feature of a corresponding positive patch w.r.t. v_i , where $\tilde{v}_0^+ = v$. Since for each training step we do not have the information of $\{\tilde{v}_i^+\}_{i=1}^N$ for v^- , we can use $-\ell(v, v^+, v^-)$ as a sample estimate for the expectation in Eq.6, by assuming a symmetric relationship among all patches: i.e. $E[\log \frac{\exp(v_i \tilde{v}_i^+)/\tau}{\frac{1}{N+1} \sum_{k=0}^N \exp(v_k \tilde{v}_k^+)/\tau}] = E[\log \frac{\exp(v_j \tilde{v}_j^+)/\tau}{\frac{1}{N+1} \sum_{k=0}^N \exp(v_k \tilde{v}_k^+)/\tau}]$, $\forall i \neq j$. Therefore, minimizing the PatchNCE loss is essentially equivalent to maximizing the variational bound of $MI(v||v^+, v^-)$.

While $MI(v||v^+)$ could potentially be increased by maximizing this lower bound of $MI(v||v^+, v^-)$, however, a direct use of the PatchNCE loss does not consider $MI(v||v^-)$ explicitly, and a unbounded $MI(v||v^-)$ may lead to sub-optimal results. Inspired by the observation that not all $\{v_n^-\}_{n=1}^N$ contribute equally to $MI(v||v^-)$ and thus the CL process, we propose to put more focuses on negative

features that potentially lead to a large $MI(v||v^-)$, which indicates these negative features are not well learnt.

Specially, we formulate the conditional probabilities as:

$$p(v||v^+) = p(v) \frac{\exp(v \cdot v^+)/\tau}{\exp(v \cdot v^+)/\tau + \sum_{n=1}^N \exp(v \cdot v_n^-)/\tau}, \quad (7)$$

$$p(v||v_n^-) = p(v) \frac{\exp(v \cdot v_n^-)/\tau}{\exp(v \cdot v^+)/\tau + \sum_{i=1}^N \exp(v \cdot v_i^-)/\tau}, \quad 1 \leq n \leq N. \quad (8)$$

We aim to replace N in Eq. 8 with a smaller value K by selecting top-ranked negative features. To this end, for the mutual information $MI(v||v^-)$, let $H(\cdot)$ denotes the entropy, then we have:

$$MI(v||v^-) = H(v) - H(v||v^-) \quad (9)$$

$$= H(v) + E_{v||v^-} [E_{v||v^-} [\log(p(v||v^-))]]. \quad (10)$$

Given v and v^- , we can use $p(v||v_n^-) \log(p(v||v_n^-))$ as a sample estimate of $E_{v||v^-} [\log(p(v||v^-))]$ for each v_n^- , $n = 1, \dots, N$. Therefore, a larger $p(v||v_n^-)$ will also lead to a larger $MI(v||v^-)$. Since $p(v||v_n^-)$ is monotonically increasing w.r.t. the similarity score $v \cdot v_n^-$ between v and v_n^- , we thus use $v \cdot v_n^-$ as the measure of the contribution of v_n^- to $MI(v||v^-)$, and construct the NCE loss by selecting the top-ranked negative features so as to focus on the potential negative features that may lead to the MI explosion.

3.4 Multi-layer Contrastive Rank

As shown in Fig. 4, a multi-layer contrastive RankNCE is used for a multi-scale training. We formulate the new multi-level loss function based on Eq. 7 and 8 is expressed by:

$$\mathcal{L}_{RankNCE}(G, X) = E_{x \sim X} \sum_{l=1}^L \sum_{s=1}^{S_l} \{p(\hat{z}_l^s | z_l^s) + p(\hat{z}_l^s | z_l^{s \setminus s})\}_L. \quad (11)$$

We use G to generate the feature vectors $\{z_l\}_L = \{(G^l(x))\}_L$, where G^l denotes the output of the l -th layer in generator, layers $l \in \{1, 2, \dots, L\}$. We refer to the corresponding patch feature as $z_l^s \in \mathbb{R}^{C_l}$, and the none-corresponding patch feature called $z_l^{s \setminus s} \in \mathbb{R}^{(S_l-1) \times C_l}$, where C_l is the number of channels in the l -th layer, S_l denotes

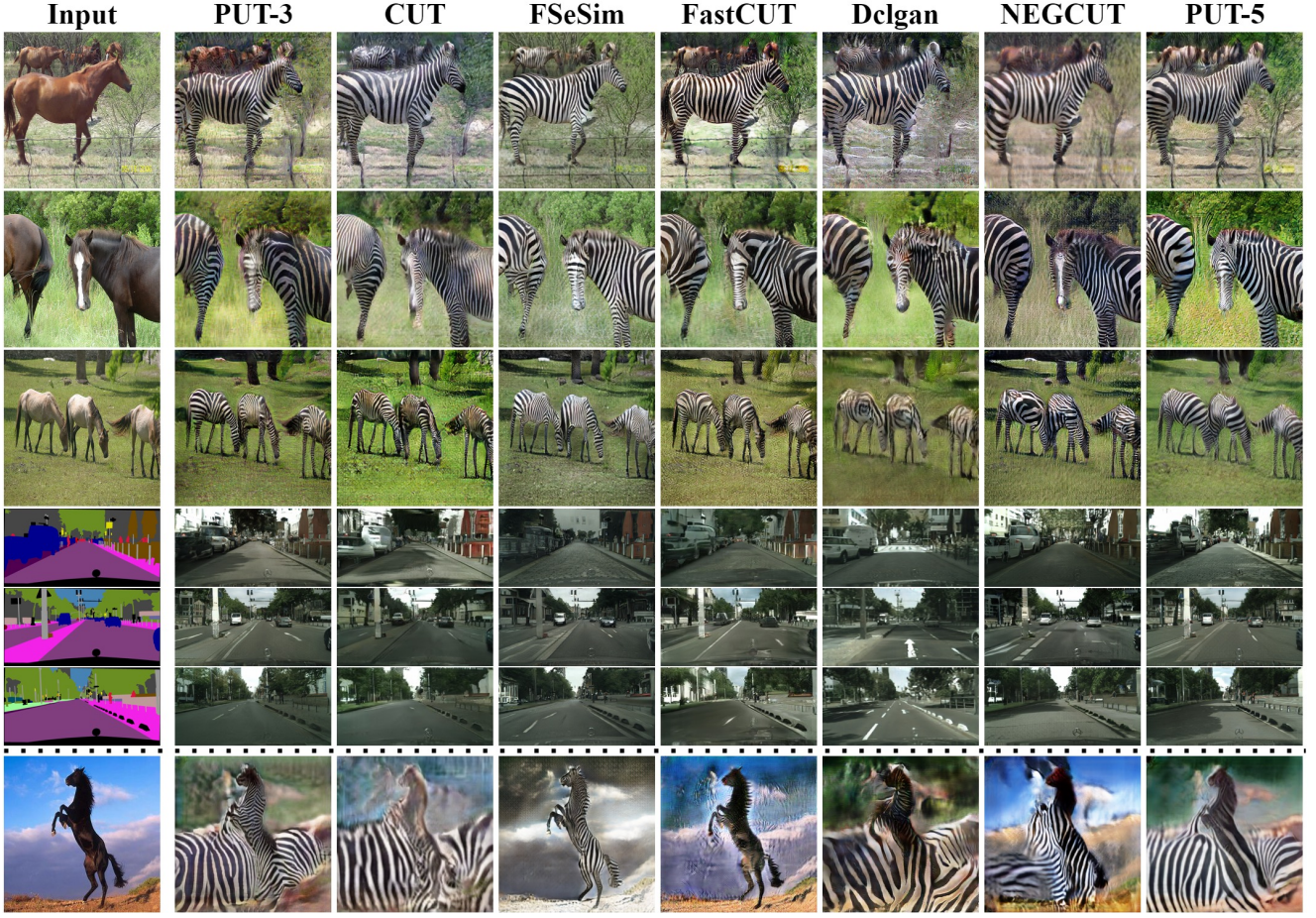


Figure 5: Qualitative results. We compare the performance of our method with state-of-the-art methods on the Horse→Zebra and CityScapes datasets, where PUT-3 and PUT-5 synthesize realistic textures with consistent structure and brightness. In particular, a typical failure case is visualized in the last row to address the limitation.

the number of spatial positions in the l -th layer, and $s \in \{1, \dots, S_l\}$. Since the corresponding patches in the real and synthesized images should share the same correspondence. Thus the RankNCE is used for identity-preserving. The overall loss is expressed as follows:

$$\mathcal{L}(G, D, X, Y) = \lambda_{GAN}(\mathcal{L}_{GAN}(G, D, X, Y) + \lambda_X \mathcal{L}_{RankNCE}(G, X) + \lambda_Y \mathcal{L}_{RankNCE}(G, Y)). \quad (12)$$

We set the $\lambda_X = 1, \lambda_Y = 1$. Compared to the previous method, our RankNCE presents a pruning strategy to select v^- for further optimization based on their contributions to $MI(v||v^-)$.

4 EXPERIMENTS

4.1 Datasets and Evaluation metrics

We evaluate our proposed method and baselines on two different datasets, i.e., the **CityScapes** [5] and **Horse→Zebra** [44] datasets. The Fréchet Inception Distance[15] (FID) is used to measure the visual quality of generated images. For the Cityscapes dataset, we obtain the segmentation mask of each method by a pre-trained DRN-32 [39] model. Then, we use mean average precision (mAp), pixel accuracy (pixAcc) and average class accuracy (classAcc) for

evaluation. We employ competitive methods for comparison, including CUT [27], Fast CUT [27], FSeSim [42], DCLGAN [12] and NEG CUT [35].

4.2 Implementation Details

We train the model for 400 epochs, and the training batchsize is 4. The learning rate is set to 0.0002, and the learning rate starts to decay linearly after half of the total epoch. Depending on the RankNCE, the number of top-ranked negative samples is set from 3 to 25 for an ablation study.

4.3 Comparison

In Tab. 1, we show a comparison of the quantitative results. Compared with current state-of-the-art methods, our approach achieves better results with competitive efficiency. For example, PUT surpasses NEG CUT with a 6.01 FID score. Compared with CUT, our model obtains a *significant improvement with similar inference speed*, that justifies the proposed algorithm is solid. As shown in Tab. 1, the semantic segmentation results on CityScapes also indicate that PUT obtains a better correspondence between output and input. As shown in Fig. 5, baseline methods produce blurry textures with

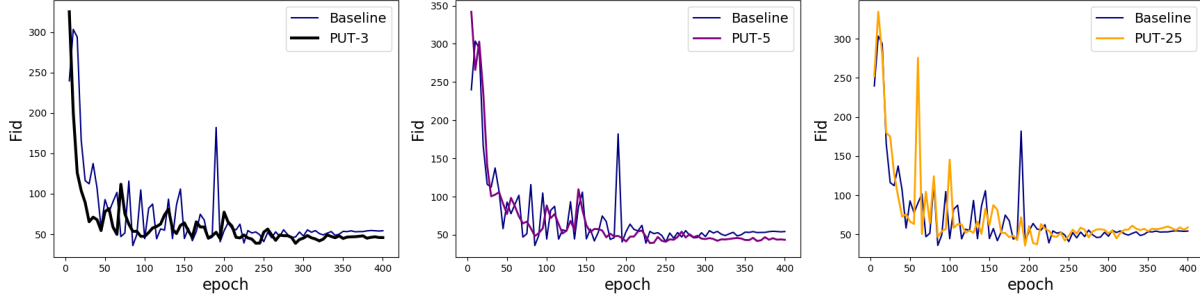


Figure 6: Training stability on Horse→Zebra. ‘PUT-K’ indicates the K number of top-ranked negative patches used in RankNCE. Better stability and superior performance are achieved by PUT with fewer negative patches.

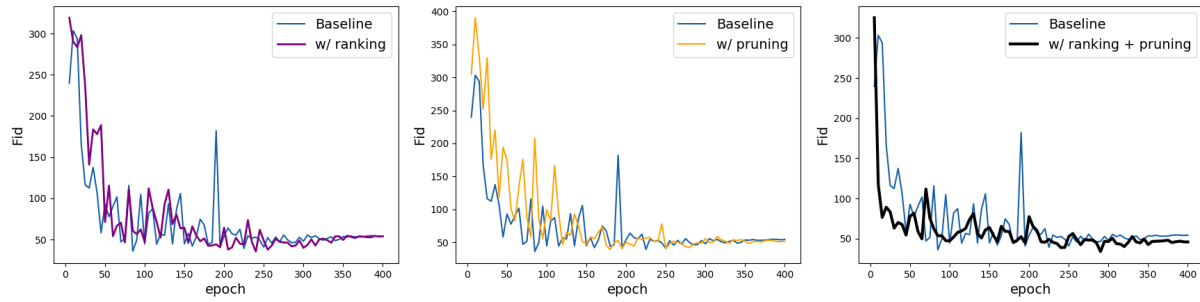


Figure 7: Ablations of RankNCE on Horse→Zebra. We use ‘sparsifying’ and ‘ranking’ sub-modules separately for ablation study.

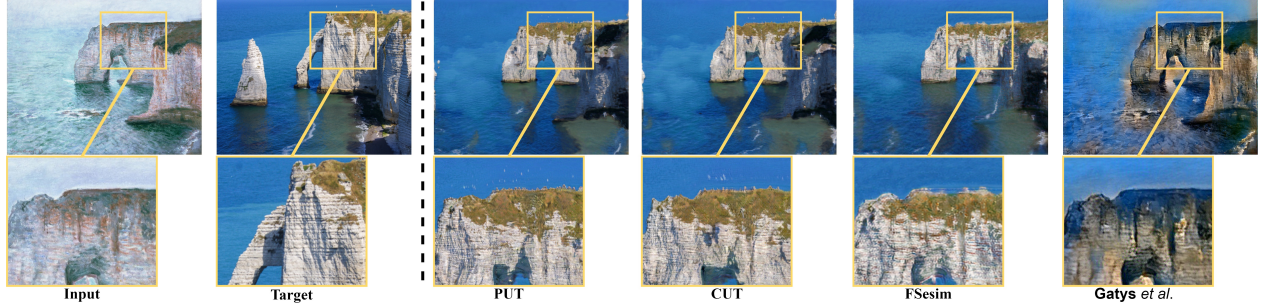


Figure 8: High-resolution effects. Our method successfully captures the style of the target image while preserving the original structure. Zooming up for a better view.

poor brightness, while PUT still synthesizes realistic textures with consistent structure and brightness toward the input image.

Stability. The most interesting part of our experiment is that PUT strengthens the stability in adversarial learning. As depicted in Fig. 6, ‘Baseline’ (i.e., CUT) gives an unstable convergence curve despite CL is used. We use top-3, top-5 and top-25 negative samples in RankNCE for comparison. To our surprise, ‘PUT-3’ and ‘PUT-5’ achieve better stability and superior performance by using fewer negative samples.

Efficiency. As shown in Tab. 1, we compare the average running time of different methods for reconstructing all images in the Horse→Zebra dataset. Compared with CUT, the proposed achieves superior results with similar efficiency. Compared with NEG CUT and DCLGan, the proposed model demonstrates better efficiency and significant performance improvements. Though our model

reaches a similar level of efficiency among state-of-the-art methods, we achieve solid performance and help to stabilize the training process. The above results show that PUT outperforms the existing models while promising competitive efficiency.

4.4 Ablations

We perform analyses to verify the effectiveness of each component in PUT, including RankNCE loss, and multi-layer RankNCE. To analyze RankNCE, we use the ‘pruning’ and ‘ranking’ sub-modules separately. In the Fig. 7, ‘w/ pruning’ show better stability with similar FID result. Though the training curve becomes more stable, a solo ranking/pruning strategy is fail to improve image quality. Then, we include ranking and pruning operations, and observe that the training curve becomes more stable and the FID is consistently improved.

Method	CityScapes				Horse→Zebra		
	mAP ↑	pixAcc ↑	classAcc ↑	FID ↓	FID ↓	Speed(s)	Memory
CUT	22.29	75.22	29.6	62.19	45.51	0.245	3.053
Fast CUT	18.05	66.63	24.2	99.18	73.37	0.150	2.573
FSeSim	19.06	66.00	26.7	51.23	43.80	0.107	2.920
DCLGan	22.91	76.97	29.6	47.83	42.64	0.389	7.014
NEGCUT	22.83	77.04	29.0	42.65	39.63	0.571	4.754
PUT-3	24.31	78.28	31.7	41.43	33.82	0.245	3.053
PUT-5	24.86	79.17	30.1	42.99	33.62	0.247	3.053

Table 1: Quantitative Comparison. Our method outperforms state-of-the-art methods across all evaluation metrics.

method	Training setting	CityScapes				Horse→Zebra	
	layer	FID ↓	pixAcc ↑	classAcc ↑	mAp ↑	FID ↓	
w/ solo RankNCE	1	42.76	30.81	76.24	24.01	41.33	
w/ Multi-layer RankNCE	5	41.43	31.71	78.28	24.31	33.82	

Table 2: Ablation on Multi-layer RankNCE.

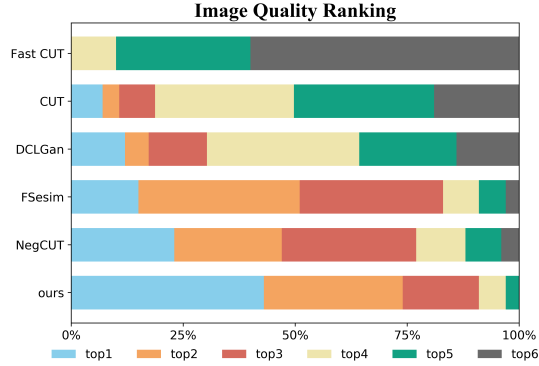


Figure 9: User study results. We conducted an in-depth quality study by ranking the user’s mean opinion score(MOS).

We conduct an ablation study of the multi-layer RankNCE, and analyze the experimental results on Horse→Zebra and CityScapes. As depicted in Tab. 2, ‘w/ Multi-layer RankNCE’ exhibits the best results on the FID index, which reveals that multi-layer RankNCE is effective for I2I translation.

4.5 User study

To further demonstrate the quality of our results, we conduct a user study according to the mean opinion score. We select 50 images randomly and forward them with baseline models to obtain the results for comparison. We recruited 10 volunteers for testing and asked volunteers to rank the results based on perception quality. As shown in Fig. 9, our method shows advantages over other methods by achieving 57% Top-1 preference.

4.6 High-Resolution Effect

To further evaluate the versatility of our algorithm, we conduct PUT for an experiment of the single image high-resolution translation, which means the source/target domain only has one picture and they are totally unpaired. In this task, we transfer Claude

Monet’s paintings to reference natural photographs by following prior works [27, 42]. Specifically, the generators and discriminators of our model are based on StyleGAN2 [20], and we use gradient penalty to stabilize optimization [25]. In particular, the RankNCE loss is used for identity-preserving.

Result. We compare our model with baseline methods including neural style transformation methods (Gatys et al [7]) and the latest single image translation methods (CUT [27] and FSeSim [42]) for a qualitative comparison. As shown in Fig. 8, our model produces a higher quality result. For example, our model successfully captures the style of the target image while preserving the structure of the input well.

5 CONCLUSION AND LIMITATIONS

In this paper, we propose a novel model called PUT for unpaired image-to-image translation. Compared with the previous contrastive learning methods, our proposed PUT is stable to learn the information between the corresponding patches, leading to a more effective contrast learning system.

However, there still exist some limitations. For instance, current image translation methods, including PUT, could fail when the given category, which is recognized as source instance, has too few pixels in the input image. How to effectively address these problems still remains an open question, which we will discuss in our future work.

REFERENCES

- [1] Kyungjune Baek, Yunje Choi, Youngjung Uh, Jaejun Yoo, and Hyunjeong Shim. 2021. Rethinking the truly unsupervised image-to-image translation. In *Proceedings of the IEEE/CVF International Conference on Computer Vision*. 14154–14163.
- [2] Sagie Benaim and Lior Wolf. 2017. One-sided unsupervised domain mapping. *Advances in neural information processing systems* 30 (2017).
- [3] Mu Cai, Hong Zhang, Huijuan Huang, Qichuan Geng, Yixuan Li, and Gao Huang. 2021. Frequency domain image translation: More photo-realistic, better identity-preserving. In *Proceedings of the IEEE/CVF International Conference on Computer Vision*. 13930–13940.
- [4] Ting Chen, Simon Kornblith, Mohammad Norouzi, and Geoffrey Hinton. 2020. A simple framework for contrastive learning of visual representations. In *International conference on machine learning*. PMLR, 1597–1607.
- [5] Marius Cordts, Mohamed Omran, Sebastian Ramos, Timo Rehfeld, Markus Enzweiler, Rodrigo Benenson, Uwe Franke, Stefan Roth, and Bernt Schiele. 2016.

- The cityscapes dataset for semantic urban scene understanding. In *Proceedings of the IEEE conference on computer vision and pattern recognition*. 3213–3223.
- [6] Huan Fu, Mingming Gong, Chaohui Wang, Kayhan Batmanghelich, Kun Zhang, and Dacheng Tao. 2019. Geometry-consistent generative adversarial networks for one-sided unsupervised domain mapping. In *Proceedings of the IEEE/CVF Conference on Computer Vision and Pattern Recognition*. 2427–2436.
 - [7] Leon A Gatys, Alexander S Ecker, and Matthias Bethge. 2016. Image style transfer using convolutional neural networks. In *Proceedings of the IEEE conference on computer vision and pattern recognition*. 2414–2423.
 - [8] Chongjian Ge, Yibing Song, Yuying Ge, Han Yang, Wei Liu, and Ping Luo. 2021. Disentangled cycle consistency for highly-realistic virtual try-on. In *Proceedings of the IEEE/CVF Conference on Computer Vision and Pattern Recognition*. 16928–16937.
 - [9] Ian Goodfellow, Jean Pouget-Abadie, Mehdi Mirza, Bing Xu, David Warde-Farley, Sherjil Ozair, Aaron Courville, and Yoshua Bengio. 2014. Generative adversarial nets. *Advances in neural information processing systems* 27 (2014).
 - [10] Michael Gutmann and Aapo Hyvärinen. 2010. Noise-contrastive estimation: A new estimation principle for unnormalized statistical models. In *Proceedings of the thirteenth international conference on artificial intelligence and statistics*. JMLR Workshop and Conference Proceedings, 297–304.
 - [11] Isma Hadji, Konstantinos G Derpanis, and Allan D Jepson. 2021. Representation learning via global temporal alignment and cycle-consistency. In *Proceedings of the IEEE/CVF Conference on Computer Vision and Pattern Recognition*. 11068–11077.
 - [12] Junlin Han, Mehrdad Shoeiby, Lars Petersson, and Mohammad Ali Armin. 2021. Dual contrastive learning for unsupervised image-to-image translation. In *Proceedings of the IEEE/CVF Conference on Computer Vision and Pattern Recognition*. 746–755.
 - [13] Kaiming He, Haoqi Fan, Yuxin Wu, Saining Xie, and Ross Girshick. 2020. Momentum contrast for unsupervised visual representation learning. In *Proceedings of the IEEE/CVF conference on computer vision and pattern recognition*. 9729–9738.
 - [14] Olivier Henaff. 2020. Data-efficient image recognition with contrastive predictive coding. In *International Conference on Machine Learning*. PMLR, 4182–4192.
 - [15] Martin Heusel, Hubert Ramsauer, Thomas Unterthiner, Bernhard Nessler, and Sepp Hochreiter. 2017. Gans trained by a two time-scale update rule converge to a local nash equilibrium. *Advances in neural information processing systems* 30 (2017).
 - [16] R Devon Hjelm, Alex Fedorov, Samuel Lavoie-Marchildon, Karan Grewal, Phil Bachman, Adam Trischler, and Yoshua Bengio. 2018. Learning deep representations by mutual information estimation and maximization. *arXiv preprint arXiv:1808.06670* (2018).
 - [17] Xun Huang, Ming-Yu Liu, Serge Belongie, and Jan Kautz. 2018. Multimodal unsupervised image-to-image translation. In *Proceedings of the European conference on computer vision (ECCV)*. 172–189.
 - [18] Phillip Isola, Jun-Yan Zhu, Tinghui Zhou, and Alexei A Efros. 2017. Image-to-image translation with conditional adversarial networks. In *Proceedings of the IEEE conference on computer vision and pattern recognition*. 1125–1134.
 - [19] Zhiwei Jia, Bodi Yuan, Kangkang Wang, Hong Wu, David Clifford, Zhiqiang Yuan, and Hao Su. 2021. Semantically Robust Unpaired Image Translation for Data with Unmatched Semantics Statistics. In *Proceedings of the IEEE/CVF International Conference on Computer Vision*. 14273–14283.
 - [20] Tero Karras, Samuli Laine, Miika Aittala, Janne Hellsten, Jaakko Lehtinen, and Timo Aila. 2020. Analyzing and improving the image quality of stylegan. In *Proceedings of the IEEE/CVF conference on computer vision and pattern recognition*. 8110–8119.
 - [21] Junho Kim, Minjae Kim, Hyeonwoo Kang, and Kwanghee Lee. 2019. U-gat-it: Unsupervised generative attentional networks with adaptive layer-instance normalization for image-to-image translation. *arXiv preprint arXiv:1907.10830* (2019).
 - [22] Gihyun Kwon and Jong Chul Ye. 2021. Diagonal attention and style-based GAN for content-style disentanglement in image generation and translation. In *Proceedings of the IEEE/CVF International Conference on Computer Vision*. 13980–13989.
 - [23] Xinyang Li, Shengchuan Zhang, Jie Hu, Liujuan Cao, Xiaopeng Hong, Xudong Mao, Feiyue Huang, Yongjian Wu, and Rongrong Ji. 2021. Image-to-image translation via hierarchical style disentanglement. In *Proceedings of the IEEE/CVF Conference on Computer Vision and Pattern Recognition*. 8639–8648.
 - [24] Ming-Yu Liu, Thomas Breuel, and Jan Kautz. 2017. Unsupervised image-to-image translation networks. *Advances in neural information processing systems* 30 (2017).
 - [25] Lars Mescheder, Andreas Geiger, and Sebastian Nowozin. 2018. Which training methods for GANs do actually converge?. In *International conference on machine learning*. PMLR, 3481–3490.
 - [26] Yingxue Pang, Jianxin Lin, Tao Qin, and Zhibo Chen. 2021. Image-to-image translation: Methods and applications. *IEEE Transactions on Multimedia* (2021).
 - [27] Taesung Park, Alexei A Efros, Richard Zhang, and Jun-Yan Zhu. 2020. Contrastive learning for unpaired image-to-image translation. In *European Conference on Computer Vision*. Springer, 319–345.
 - [28] Taesung Park, Ming-Yu Liu, Ting-Chun Wang, and Jun-Yan Zhu. 2019. Semantic image synthesis with spatially-adaptive normalization. In *Proceedings of the IEEE/CVF conference on computer vision and pattern recognition*. 2337–2346.
 - [29] Ben Poole, Sherjil Ozair, Aaron Van Den Oord, Alex Alemi, and George Tucker. 2019. On variational bounds of mutual information. In *International Conference on Machine Learning*. PMLR, 5171–5180.
 - [30] Elad Richardson, Yuval Alaluf, Or Patashnik, Yotam Nitzan, Yaniv Azar, Stav Shapira, and Daniel Cohen-Or. 2021. Encoding in style: a stylegan encoder for image-to-image translation. In *Proceedings of the IEEE/CVF Conference on Computer Vision and Pattern Recognition*. 2287–2296.
 - [31] Xuning Shao and Weidong Zhang. 2021. SPatchGAN: A Statistical Feature Based Discriminator for Unsupervised Image-to-Image Translation. In *Proceedings of the IEEE/CVF International Conference on Computer Vision*. 6546–6555.
 - [32] Aaron Van den Oord, Yazhe Li, Oriol Vinyals, et al. 2018. Representation learning with contrastive predictive coding. *arXiv preprint arXiv:1807.03748* 2, 3 (2018), 4.
 - [33] Tongzhou Wang and Phillip Isola. 2020. Understanding contrastive representation learning through alignment and uniformity on the hypersphere. In *International Conference on Machine Learning*. PMLR, 9929–9939.
 - [34] Ting-Chun Wang, Ming-Yu Liu, Jun-Yan Zhu, Andrew Tao, Jan Kautz, and Bryan Catanzaro. 2018. High-resolution image synthesis and semantic manipulation with conditional gans. In *Proceedings of the IEEE conference on computer vision and pattern recognition*. 8798–8807.
 - [35] Weilun Wang, Wengang Zhou, Jianmin Bao, Dong Chen, and Houqiang Li. 2021. Instance-wise Hard Negative Example Generation for Contrastive Learning in Unpaired Image-to-Image Translation. In *Proceedings of the IEEE/CVF International Conference on Computer Vision*. 14020–14029.
 - [36] Yaxing Wang, Héctor Laria, Joost van de Weijer, Laura Lopez-Fuentes, and Bogdan Raducanu. 2021. TransferI2I: Transfer Learning for Image-to-Image Translation from Small Datasets. In *Proceedings of the IEEE/CVF International Conference on Computer Vision*. 14010–14019.
 - [37] Shaoan Xie, Mingming Gong, Yanwu Xu, and Kun Zhang. 2021. Unaligned image-to-image translation by learning to reweight. In *Proceedings of the IEEE/CVF International Conference on Computer Vision*. 14174–14184.
 - [38] Zili Yi, Hao Zhang, Ping Tan, and Minglun Gong. 2017. Dualgan: Unsupervised dual learning for image-to-image translation. In *Proceedings of the IEEE international conference on computer vision*. 2849–2857.
 - [39] Fisher Yu, Vladlen Koltun, and Thomas Funkhouser. 2017. Dilated residual networks. In *Proceedings of the IEEE conference on computer vision and pattern recognition*. 472–480.
 - [40] Fangneng Zhan, Yingchen Yu, Kaiwen Cui, Gongjie Zhang, Shijian Lu, Jianxiong Pan, Changgong Zhang, Feiyang Ma, Xuansong Xie, and Chunyan Miao. 2021. Unbalanced feature transport for exemplar-based image translation. In *Proceedings of the IEEE/CVF Conference on Computer Vision and Pattern Recognition*. 15028–15038.
 - [41] Wenlong Zhang, Yihao Liu, Chao Dong, and Yu Qiao. 2019. Ranksrgan: Generative adversarial networks with ranker for image super-resolution. In *Proceedings of the IEEE/CVF International Conference on Computer Vision*. 3096–3105.
 - [42] Chuanxia Zheng, Tat-Jen Cham, and Jianfei Cai. 2021. The spatially-correlative loss for various image translation tasks. In *Proceedings of the IEEE/CVF Conference on Computer Vision and Pattern Recognition*. 16407–16417.
 - [43] Xingran Zhou, Bo Zhang, Ting Zhang, Pan Zhang, Jianmin Bao, Dong Chen, Zhongfei Zhang, and Fang Wen. 2021. Cocosnet v2: Full-resolution correspondence learning for image translation. In *Proceedings of the IEEE/CVF Conference on Computer Vision and Pattern Recognition*. 11465–11475.
 - [44] Jun-Yan Zhu, Taesung Park, Phillip Isola, and Alexei A Efros. 2017. Unpaired image-to-image translation using cycle-consistent adversarial networks. In *Proceedings of the IEEE international conference on computer vision*. 2223–2232.